International Journal of Applied Science and Engineering

Influences of high-volume fly ash and bottom ash as feldspar replacements on eco-friendly ceramic building materials

Ming-Gin Lee [1*], Wei-Chien Wang [2], Yishuo Huang [1], Tai-Mi Lee [2], Yung-Chih Lin [2]

[1] *Department of Construction Engineering, Chaoyang University of Technology, Taichung 413310, Taiwan*
[2] *Department of Civil Engineering, National Central University, Taoyuan 320, Taiwan*

ABSTRACT

Fly ash and bottom ash in concrete have been extensively studied for decades. Nevertheless, there are few studies on applying fly ash and bottom ash in ceramic building materials, especially in the literature on physical properties and thermal shock resistance. So far, a large amount of bottom ash is buried every year. In this study, the by-products of thermal power plants, which include coal-fired fly ash and bottom ash, are used to replace 10%, 20%, 30%, 40%, 50%, and 60% of the weight of the ceramic raw material (feldspar) to produce ceramic building materials. The sintering temperature ranges from 1100 to 1200°C. Various tests were conducted to determine their performance and thermal shock resistance. According to the test results, the high-volume fly ash and bottom ash samples can be sintered into facing bricks after high-temperature sintering. The shrinkage rate decreases with the amount of addition, reducing volume loss. Warping meets the flatness specification, bending strength far exceeds the standard requirement, and no defects occur after the thermal shock resistance test. The color becomes increasingly saturated in brown with the amount of addition. These results demonstrate that coal ash can be sintered into building ceramics that meet the specification requirements. This suggests that manufacturing fired ceramic building materials using 10% to 60% coal ash is one of the sustainable recycling methods.

Keywords: Bending strength, Building ceramics, Bottom ash, Fly ash, Thermal shock resistance.

OPEN ACCESS

Received: September 29, 2023
Revised: February 12, 2024
Accepted: February 16, 2024

Corresponding Author:
Ming-Gin Lee
mglee@cyut.edu.tw

Publisher:
Chaoyang University of Technology
ISSN: 1727-2394 (Print)
ISSN: 1727-7841 (Online)

1. INTRODUCTION

As the world's economy has grown dramatically, so has electricity consumption (Glymond et al., 2018; Dagnew and Hunachew, 2022). Taiwan's demand for industrial electricity and electricity consumption for people's livelihood has also increased with the development of industry and the improvement of quality of life. Electricity generation in Taiwan can be divided into renewable energy, thermal power generation and nuclear power generation. Among them, the fuel used by thermal power plants is divided into coal, oil and natural gas (Nicoletti et al., 2002; Almeida et al., 2016).

Coal is currently an important fuel source globally (Caglayan and Caliskan, 2018; Türkmen et al., 2021). Coal-fired power plants are the main source of electricity in most countries, accounting for about 27% of global power generation, the largest single power generation category in the world (Vieira et al., 2023). In addition, this proportion is likely to continue to rise in 2022. Because European countries need to make up for Russia and Ukraine in the short-term Hydropower shortages caused by post-war drought and soaring gas prices. In Germany alone 3.2GW of coal-fired capacity has been restarted, and it is expected that Germany will add another 5.5GW of coal-fired capacity by the end of the year, according to BloombergNEF (BNEF). However, BNEF notes that while the proportion of coal-fired power generation in Europe has increased, it mainly comes from China, India and the United States, accounting for 63% of the total coal-fired power generation. Among them, China accounts for 52% of the world's total coal consumption, India and the United States account for 11% and 9% respectively, and the remaining seven large coal-fired countries are Japan, South Korea, Indonesia, South Africa, Germany, Russia and Australia, accounting for coal-fired power generation (Vieira et al., 2023). Coal-fired ash, an industrial by-product produced during the combustion of coal, has currently estimated to be around 400 million tons per year (Eduardo et al., 2018; Ngayakamo et al., 2020) and continues to grow as electricity demand grows. A large amount of industrial waste can cause serious environmental and ecological problems if not handled properly. Due to its ecological and economic importance, the potential reuse and efficient use of this waste has being investigated around the world (Ye et al., 2018; Zhang and Biswas, 2021).

Taipower's coal-fired power plants produce nearly 2 million metric tons of coal ash every year. How to properly handle the by-products of coal combustion has become an important issue, and the annual coal ash production has increased year by year. Taiwan is densely populated and has limited land. The increasing waste production year by year makes landfills gradually overwhelmed, and waste disposal costs are high. In recent years, the issues of environmental protection and energy conservation have generally received attention. How to reduce energy use and the impact on the environment is currently a goal that is being actively promoted internationally. Nowadays, all countries in the world are actively researching various energy-saving materials, hoping to reduce the impact on the environment. Among construction materials, the production of ceramic facing bricks requires a large amount of clay materials (Bovea et al., 2007; Babisk et al., 2020). However, Taiwan currently has no clay materials and almost relies on imported natural materials. In addition to the relatively high cost, natural materials will also be exhausted due to continuous large-scale use. In recent years, there are few research reports on the use of coal-fired ash to produce ceramics (Zimmer and Bergmann, 2007; Namkane et al., 2017). The results are encouraging, and it is found that the glass-ceramic produced from fly ash is a harmless and valuable material with broad application prospects during the high-temperature vitrification and subsequent heat treatment of nucleation and crystallization. In addition, there is research (Vilarinho et al., 2022) on the development of ecological ceramic wall tiles using biological calcium carbonate in eggshell waste as raw material. There are studies (Menezes et al., 2005; Souza et al., 2010) on the use of granite sawing waste to produce ceramic tiles. Some studies (Namkane et al., 2017; Asensio et al., 2020) have used weathered lignite and coal bottom ash to produce ceramic floor tiles. Some studies (Sokolar and Smetanova, 2010; Húlan et al., 2020) have used mineral fly ash as a raw material for tiles. There are studies (Gabaldón et al., 2014; Kummoonin et al., 2014) on the use of industrial waste to manufacture ceramic floor tiles. There are studies (Schabbach et al., 2012; Taurino et al., 2017) on the use of clay and municipal solid waste incineration bottom ash mixture to produce ceramics, etc.

The main purpose of this research is to make the power plant coal-fired fly ash and bottom ash can be effectively used in ceramic buildings, especially the reuse of bottom ash is important, from the exploration of coal ash and bottom ash to replace part of clay (10%, 20%, 30%, 40%, 50%, and 60%) to prepare ceramic mixture. After ingot casting and sintering, its performance and thermal shock resistance were tested to evaluate its feasibility.

2. MATERIALS AND METHODS

In this study, the by-products of thermal power plants, namely, coal-fired fly ash and bottom ash, were employed to replace the ceramic tile raw materials by weight in proportions of 10%, 20%, 30%, 40%, 50%, and 60%. Subsequently, the ingot casting and sintering procedures were conducted at a sintering temperature of 1100°C, resulting in the creation of recycled ceramic tiles. To evaluate the properties of these tiles, various tests were performed according to the national standard CNS 9737 for ceramic tiles. These tests included assessments of water absorption, appearance size, shrinkage, warpage, bending strength, and visual inspection. Furthermore, comparisons were made between the test results for ceramic bricks with coal-fired fly ash and bottom ash. The experimental materials and methods are described in detail below, and a flowchart illustrating the process of producing coal ash recycled ceramic tiles is provided in Fig. 1.

2.1 Raw Material

The experimental materials and preparation used in this study are as follows:

(1) Ceramic tile raw material: The raw materials of ceramic tiles in this research are from Leiying Co., Ltd., including albite, potassium feldspar, ball clay, kaolin, and quartz. The chemical composition is shown in Table 1.

(2) Coal fly ash: Coal-fired fly ash in power plants is yellow-brown powder. Due to the formation method and collection method, the fly ash has reached the fine particle size. After collection, it is dried at 105 ± 5°C. After drying, it is stored in a dry and moisture-proof manner, and it is dried before use. Its chemical composition analysis is shown in Table 2, and the appearance photos are shown in Fig. 2(a).

(3) Coal bottom ash: The coal bottom ash of the power plant is black and dark brown regular lumps. Because the state is irregular in size, it is dried at 105 ± 5°C after collection. After drying, it is preliminarily crushed and passed through a #4 sieve for use. After undergoing crushed with a disk mill and grinding with a ball mill, the particles that pass through a #200 sieve are collected as powder, and dried before use. Its chemical composition analysis is shown in Table 2, and the appearance photos are shown in Fig. 2(b) and 2(c).

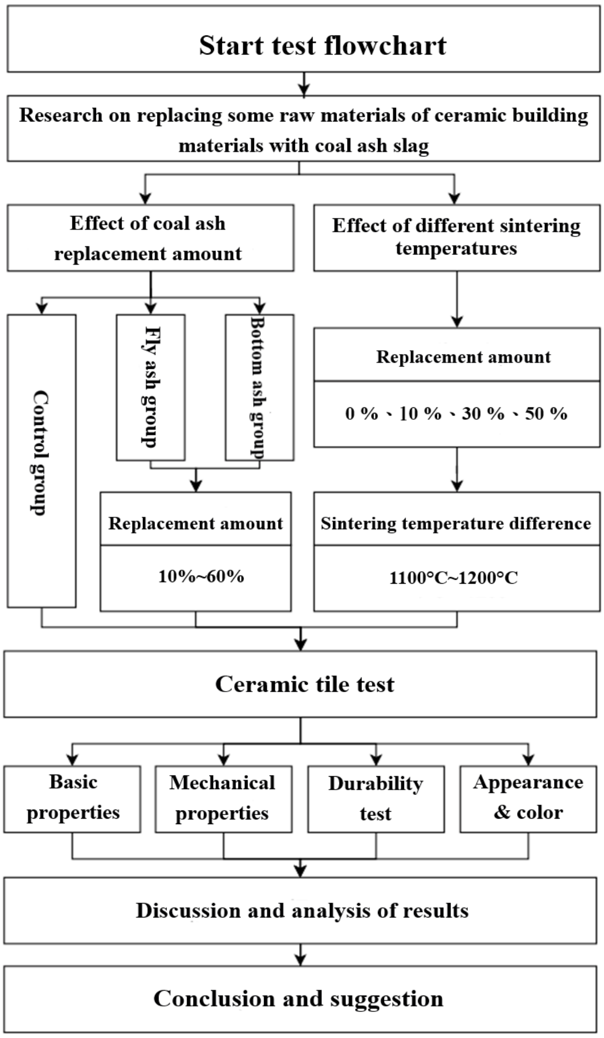

Fig. 1. Test flowchart of coal ash recycled ceramic tile

2.2 Test Specimens and Test Methods

2.2.1 Ingot making of test specimen

After drying all the raw materials for the test, weigh the required weight, add an appropriate amount of water and mix evenly, then dry, grind and sieve to complete the powder preparation. Weigh the powder required for a single test sample and add 10% water to stir evenly to help shape. Pour the powder into the assembled mold as shown in Fig. 3(a); use a tamping stick to tamp the powder slightly as shown in Fig. 3(b); then move the mold filled with powder to Pressurize the hydraulic press machine repeatedly 3 times as shown in Fig. 3(c); take out the base and top cover, place the retaining ring and top block on the top and bottom of the mold as shown in Fig. 3(d), and move to the hydraulic press Pressurize the machine to eject the test sample, and complete the ingot pressing of the test sample as shown in Fig. 3(e). Among them, the ingot mold is shown in Fig. 4(a), and the embryo is ejected from the test mold as shown in Fig. 4(b).

2.2.2 Temperature curve

After the ingot pressing of the test specimen is completed, it is dried in an oven and sent to a furnace for high-temperature sintering. The heating program and temperature curve are adjusted according to the results of the previous study. Finally, the sintering temperature curve of this study was finally divided into four stages according to the test results, and the firing was completed after 7 h. The temperature curve is shown in Fig. 5.

(1) Low temperature stage: the heating rate was 9°C/min from room temperature to 300°C, and the temperature was maintained at 300°C for 60 min.
(2) Medium temperature stage: 4.4°C/min heating rate from 300 to 700°C, and maintain the temperature at 700°C for 30 min.
(3) High temperature stage: 4.4°C/min from 700 to 1100°C. The temperature was maintained at 1100°C for 120 min.
(4) Cooling stage: take out the test after cooling down to room temperature naturally.

Table 1. Chemical composition of ceramic tile raw materials（%）

Composition	SiO_2	Al_2O_3	Fe_2O_3	CaO	MgO	K_2O	Na_2O	Loss on ignition
Potassium feldspar	65.45	19.13	0.14	0.07	0.10	12.09	2.65	0.28
Albite	68.56	18.16	0.11	0.16	0.03	0.54	10.82	0.15
Ball clay	47.01	36.24	0.89	0.01	0.17	0.70	0.06	14.60
Kaolin	44.50	39.50	0.50	0.05	0.07	0.04	0.52	13.60
Quartz	100	—	—	—	—	—	—	—

Table 2. Chemical composition of coal fly ash and bottom ash (%)

Composition	SiO_2	Al_2O_3	Fe_2O_3	CaO	MgO	K_2O	Na_2O	Loss on ignition
Coal fly ash	61.5	19.1	7.65	5.44	2.80	1.04	1.16	0.53
Coal bottom ash	53.7	17.6	9.34	6.34	2.32	0.89	1.06	4.73

Lee et al., International Journal of Applied Science and Engineering, 21(2), 2023397

(a) (b) (c)

Fig. 2. Coal fly ash and bottom ash (a) fly ash (b) bottom ash before grinding (c) bottom ash after treatment

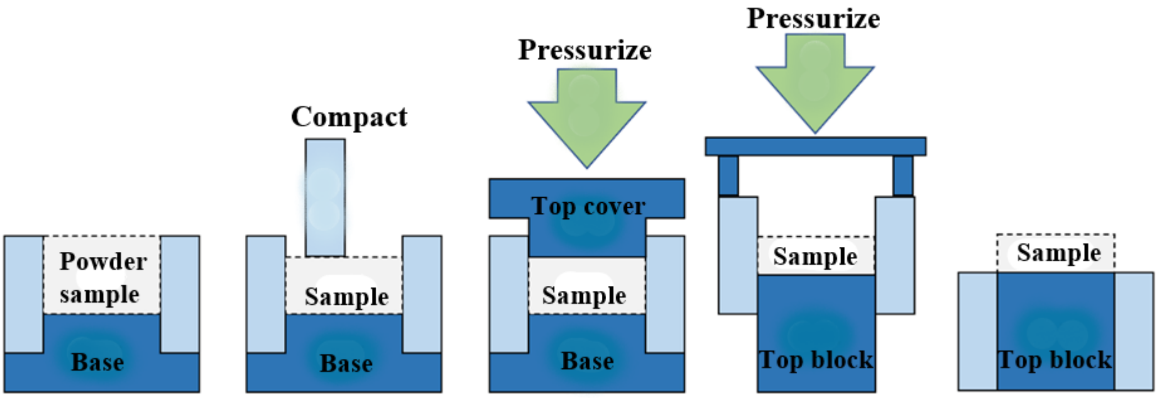

(a) (b) (c) (d) (e)

Fig. 3. Schematic diagram of test sample ingot (a) filling in sample (b) pre-tamping (c) pressurization (d) jacking out (e) sample remove

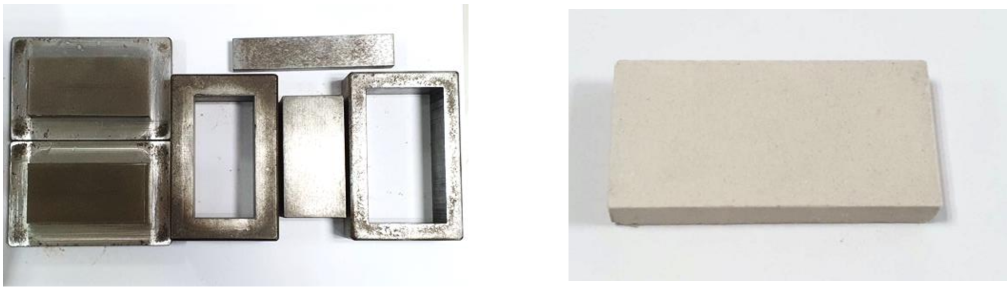

(a) (b)

Fig. 4. (a) Ingot mold photo (b) embryo photo

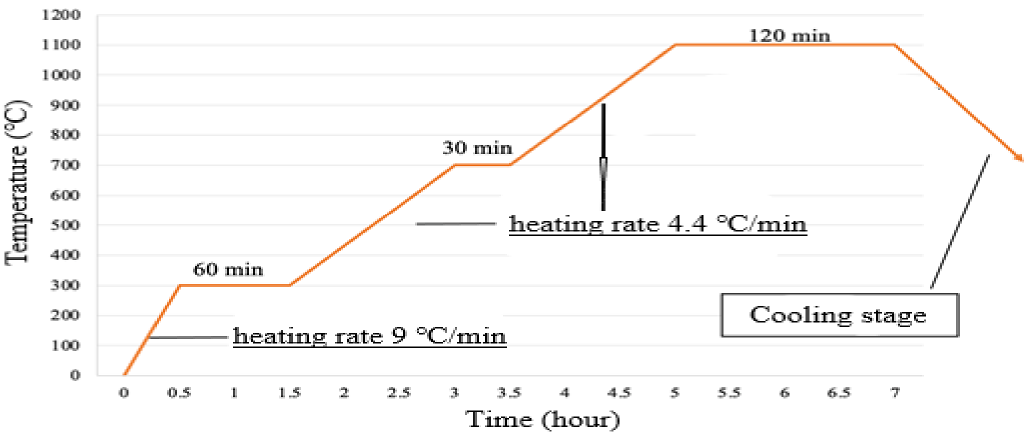

Fig. 5. Sintering time and temperature curve

2.2.3 Proportioning design

In order to explore the different results of different substitution ratios of coal-fired ash, the meaning of the test coding is explained as follows. In this study, only the feldspar group and the clay group are replaced in the 95% of the ceramic tile composition. FA and BA represent that the test sample uses coal-fired fly ash and bottom ash as replacement materials respectively. The number takes 10-FA as an example. This test sample uses coal-fired fly ash to replace the feldspar and clay in the raw material of ceramic tiles. Accounting for 10% of 95%, the total substitution amount is 9.5% of the total weight of the control group. The test code and proportioning design are shown in Table 3. After the ceramic test sample is sintered, it will be tested according to the national standard CNS 9737 "Ceramic Brick", such as water absorption, appearance size, shrinkage, warpage, bending test and other items. The relevant test items are described in the following sections.

2.2.4 Water absorption test

Determination of the quality of water absorption according to the boiling method test description is as follows:

(a) The samples are not in contact with each other, placed in the boiling device slightly vertically, and the distance from the bottom of the boiling device is more than 50 mm.
(b) Fill with water until the sample is submerged more than 50 mm below the water surface.
(c) Heat until the water boils, and then maintains this state for 2 h after boiling. During heating, the sample must be maintained at a state of more than 50 mm below the water surface.
(d) After 2 h, cut off the heat source, still completely immerse the sample in water, and let it stand for more than 12 h until it is slightly room temperature.
(e) Take the sample out of the boiling device, quickly wipe the surface, back and side of the sample with a damp cloth wrung out vigorously, and immediately measure the mass with a balance, and the measured value is taken as the mass when it absorbs water. When the surface is uneven, wipe it gently with a dry damp cloth.
(f) Calculate the average value of water absorption from the experimental results.

2.2.5 Surface warping test

Warping is an important test basis for the flatness of ceramic tiles. In the inspection and specification of ceramic tiles, there are different tolerances for flatness according to the size of the finished product. The larger the finished tile, the higher the tolerance. For example, the more serious the warping of ceramic tiles, the poorer the flatness when they are collaged on the exterior. In addition to the unsightly appearance, there will be safety concerns such as scratches and cracks. The surface warping test description is as follows:

(1) Surface warping as shown in Fig. 6. Set up base point 1 and base point 2 at the position about 5 mm inside the two corners on the diagonal line of the surface brick, and measure the vertical distance to the surface of the brick from the midpoint of the straight line connecting the two base points.
(2) At this time, the positive sign (+) is used for convex warping, and the negative sign (-) is used for concave warping.
(3) This measurement must be carried out on two diagonal directions, and the absolute value of the two values that is larger is used as the average value of the measured value of surface warpage to calculate the absolute value.
(4) Not applicable to face bricks whose sides are less than 50 mm and face bricks whose surface is deliberately made convex and concave.

Table 3 Test code and proportioning design (%)

Test code	Fly ash	Bottom ash	F-Feldspar 60%		C- Clay 35%		Quartz 5%
			Potassium feldspar	Albite	Ball soil	Kaolin	
Control	-	-	15	45	10	25	5
10-FA	9.5	-	13.5	40.5	9	22.5	5
20-FA	19	-	12	36	8	20	5
30-FA	28.5	-	10.5	31.5	7	17.5	5
40-FA	38	-	9	27	6	15	5
50-FA	47.5	-	7.5	22.5	5	12.5	5
60-FA	57	-	6	18	4	10	5
10-BA	-	9.5	13.5	40.5	9	22.5	5
20-BA	-	19	12	36	8	20	5
30-BA	-	28.5	10.5	31.5	7	17.5	5
40-BA	-	38	9	27	6	15	5
50-BA	-	47.5	7.5	22.5	5	12.5	5
60-BA	-	57	6	18	4	10	5

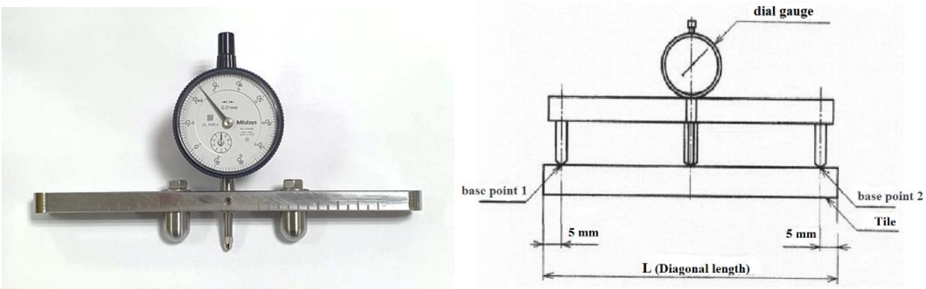

Fig. 6. Diagram of the measurement method of surface warping

2.2.6 Bending failure load test

Ceramic facing tiles are brittle materials, so the tensile strength will not be tested, but the strength of the ceramic facing tiles will be judged by the bending strength. The test method is to use the base to apply force on the brick surface at three points. The test device (refer to Fig. 7), calculate the bending failure load and bending strength through the formula.

Bending failure load: The bending failure load (S) is calculated according to Equation (1).

$$S = \frac{\mathrm{FL}}{\mathrm{b}} \quad (1)$$

In the formula, S: bending failure load (N), F: damage load (N), L: span between supporting rods (mm), b: width of sample (mm).

Bending strength: The bending strength (R) is calculated according to Equation (2).

$$R = \frac{3\mathrm{FL}}{2\mathrm{b}h^2} = \frac{3\mathrm{S}}{2h^2} \quad (2)$$

In the formula, R: bending strength (N/mm^2), F: damage load (N), L: span between supporting rods (mm), b: width of sample (mm), h: thickness of the thinnest part of the broken surface (mm).

2.2.7. Thermal shock resistance test

In the thermal shock resistance test, after the ceramic tiles are dyed, it is confirmed that there is no defect in the specimen. After drying to a high temperature of more than 100°C, the specimen is immediately placed in cold water and stirred, and it experiences a temperature of 110°C in a very short period of time. Take it out after 30 min, and then stain it again to confirm that there is no defect on the surface of the ceramic tile specimen. The purpose of the test is to understand the thermal shock resistance of the sintered specimen, evaluate the adaptability of the specimen under extreme temperature changes, and evaluate the durability of the specimen.

3. RESULTS AND DISCUSSION

In this test, the coal-fired ash from Taichung thermal power plant was used, and the ratio of feldspar and clay raw materials that replaced some ceramic materials was replaced by weight ratio of 10%, 20%, 30%, 40%, 50%, and 60%, and then 1100°C high temperature sintering. According to the basic and physical characteristics, the test of ceramic tiles is carried out, and the results are explained in the following sections.

3.1. Appearance and Morphology

There are roughly two observation methods for the description of the appearance of ceramic tile specimens with different amounts of coal-fired ash sintered after high-temperature sintering. One is visual observation, which mainly describes the appearance, deformation, cracks and other defects visible to the naked eye such as color, shape and texture. The other is to use an optical microscope to shoot the surface of the tile specimen, and observe the surface structure of the test specimen through the captured image for appearance analysis. Fig. 8 is the appearance photo of the ceramic tile samples with different fly ash substitution amount. From the apparent photos, it can be seen that the color of the tile sample changes from the off-white color of the control group to wheat color (replacing 10% of the fly ash), and turns to brown as the replacement increases to 30%. Finally, a saturated brown color is reached when the substitution reaches 60%. Fig. 9 is the optical microscope photo of the ceramic tile samples with different fly ash substitution amount. The semi-ceramic crystalline reflection can be seen in the photo. From the photos, it can be seen that the color of the tile sample changes from the off-white color of the control group to light grayish brown (replacing 10% of the fly ash), and turns to light brown as the replacement increases to 30%. When the substitution amount reaches 60%, the main color of the image is brown, with white, brown, and dark red crystals mixed in it. The appearance and optical microscope photos of the ceramic tile specimens with different amounts of bottom ash replaced are almost the same as those replaced by fly ash. And with the increase of bottom ash replacement amount, the roughness becomes more and more obvious.

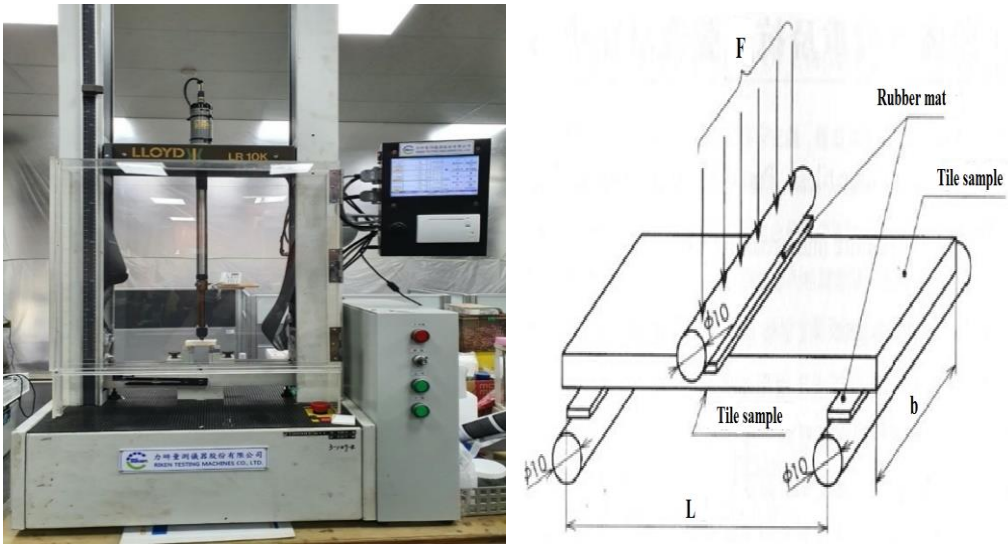

Fig. 7. Bending failure load and bending strength test device

(a) Control (b)10-FA (c)20-FA (d)30-FA (e)40-FA (f)50-FA (g)60-FA

Fig. 8. Appearance photos of ceramic tile samples with different amounts of fly ash replaced

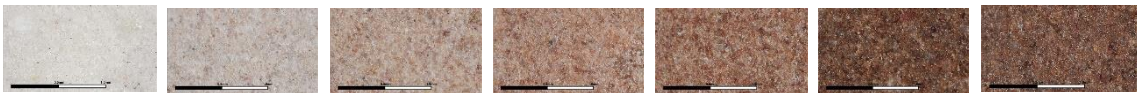

(a) Control (b)10-FA (c)20-FA (d)30-FA (e)40-FA (f)50-FA (g)60-FA

Fig. 9. Optical microscope photos of ceramic tile samples with different amounts of fly ash replaced

3.2. Results of Water Absorption Test

Fly ash or bottom ash is replaced by 10% to 60% of the raw materials of ceramic tiles, and the test sample is sintered at a high temperature of 1100℃. The water absorption test is carried out in accordance with CNS 3299-3, and the water absorption rate is detected by the boiling method. The test sample was boiled continuously for 2 h in boiling water to force the moisture into the open pores of the sample. The average water absorption rate of each fly ash ceramic tile is shown in Fig. 10(a). The average water absorption rate of each bottom ash ceramic tile is shown in Fig. 10(b). From Fig. 10(a) and (b), it can be seen that the influence of the ceramic tile with the amount of bottom ash substitution on the water absorption tends to increase, but the amount of fly ash substitution stays at 30% and no longer increases. Sokolar and Smetanova (2010) conducted a study on the impact of fly ash on ceramics fired at 1080℃. Their findings indicate that fly ash results in decreased strength, increased shrinkage after firing, and elevated water absorption levels, demonstrating similar conclusions.

3.3. Results of Scale Shrinkage Test

According to the CNS 3299-2 ceramic tile test method, the surface quality and scale shrinkage unevenness are measured with a vernier caliper, and the minimum scale of the record is 0.1 mm. As shown in Fig. 11, it can be seen that the shrinkage rate of the bottom ash recycled ceramic tile specimen decreases with the increase of the replacement amount, indicating that the replacement of the bottom ash is helpful for volume stability. However, the shrinkage rate of fly ash regenerated ceramic tiles is lower and the volume stability is more stable. When the replacement amount reaches 30% to 60%, the shrinkage rate curve slows down. The possible reason behind this phenomenon is attributed to the higher temperatures during fly ash generation conditions. A higher temperature is necessary to facilitate the sintering reaction, especially under conditions of increased substitution amounts. Consequently, the volume shrinkage of particles that have not yet participated in the melting process becomes smaller, resulting in a significant reduction in the overall volume shrinkage change when the substitution amount exceeds 20% Húlan et al. (2020). Fig.

12 illustrates the correlation between shrinkage and water absorption for fly ash or bottom ash tiles. A linear negative correlation is evident, with an R^2 value of 0.8249. Shrinkage decreases with increasing fly ash or bottom ash content, while water absorption increases in turn.

3.4. Results of Surface Warping Test

Surface warping is an important test basis for the flatness of ceramic tiles. The specifications of ceramic facing tiles have different warpage tolerances according to the size. The size of the ceramic tiles in this study is 70 × 35 × 10 mm. Using fly ash or bottom ash to replace 10% to 60% of the raw materials of ceramic tiles, under the environment of sintering temperature 1100°C, the surface warpage measurement results are shown in Table 4. The average value of the warpage of the fly ash-recycled ceramic tile specimens is between 0 and 0.06 mm, the maximum value is between 0 and 0.4 mm, and the minimum value is between 0 and -0.24 mm. The specimens substituted with

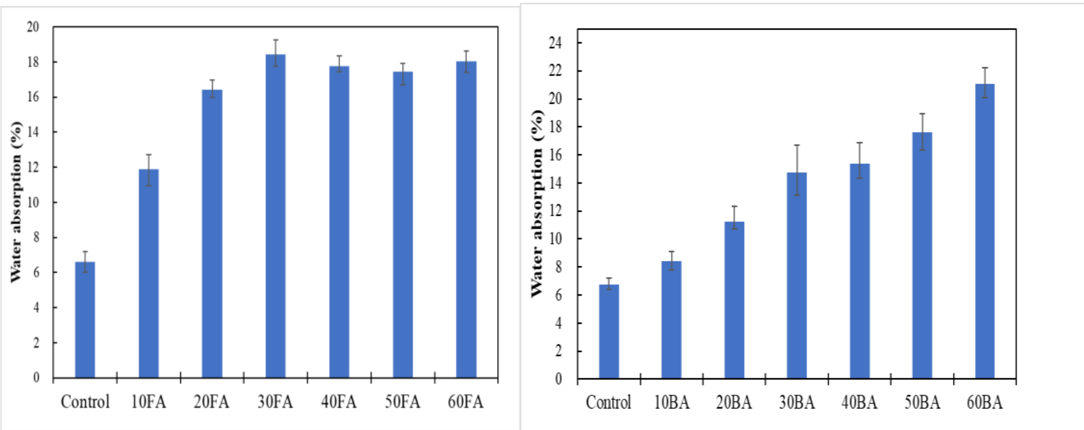

(a) (b)

Fig. 10. Average water absorption rate of (a)fly ash (b) bottom ash ceramic tile

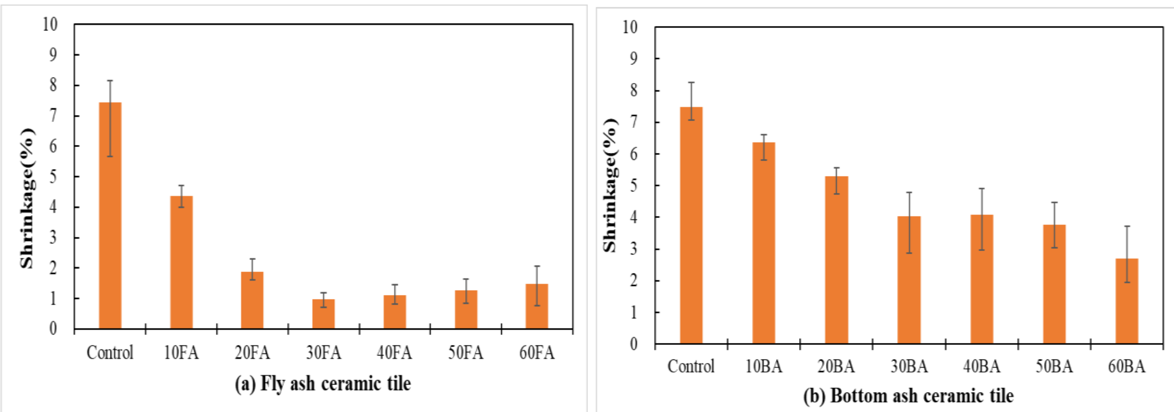

Fig. 11. Average scale shrinkage of fly ash bottom ash ceramic tile

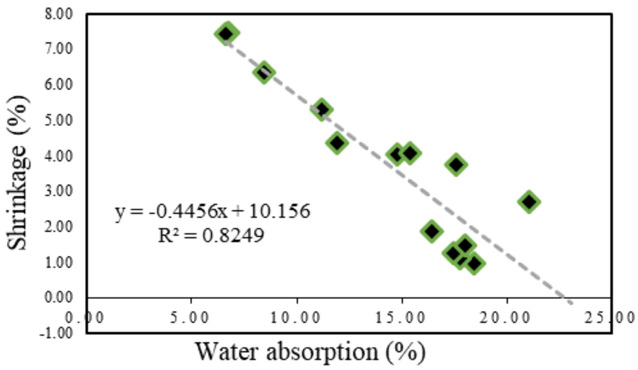

Fig. 12. Correlations between shrinkage and water absorption of fly ash or bottom ash ceramic tile

fly ash were all higher than the control group after passing through 1100°C, but they could still meet the warping ceramic tile specifications for interior and exterior ceramic tiles. It shows that when the sintering temperature is 1100°C, the flatness of the fly ash regenerated ceramic tile specimen is sufficient, and it can be installed in most positions. The warpage of the bottom ash recycled ceramic tile specimens was relatively large, with an average value between 0.38 and -0.29 mm, but all the specimens could meet the specifications for interior and exterior warping ceramic tiles.

Table 4. Surface warpage of coal ash recycled ceramic tile (unit: mm)

Test code	|Mean|	Max	Min
control	0.02	0.15	-0.14
10FA	0.06	0.4	-0.24
20FA	0.04	0.24	-0.16
30FA	0.05	0.16	-0.06
40FA	0.04	0.14	-0.04
50FA	0.06	0.16	-0.08
60FA	0.04	0.12	-0.03
10BA	0.06	0.24	-0.1
20BA	0.07	0.33	-0.24
30BA	0.06	0.38	-0.29
40BA	0.07	0.38	-0.2
50BA	0.07	0.36	-0.24
60BA	0.06	0.34	-0.21

3.5. Results of Bending Strength Test

Parts of the raw materials of ceramic tiles were replaced by coal ash by 10% to 60%. Under the environment of sintering temperature of 1100°C, the specimens of coal ash ceramic tiles were tested for bending strength according to CNS 9737 R1018. Apply a load to the specimen at a rate of 1.2 N/mm^2 per second, and measure the failure load. The results of the bending strength test for coal-ash recycled ceramic tile are shown in Table 5. It can be seen from Table 5 that when fly ash is used to replace the components of ceramic tiles, when the replacement amount reaches 30%, the bending strength is reduced by 48% compared with the control group. However, with the increase of fly ash replacement amount, it increases to 40% to 60%, close to the flexural strength of the control group. It was also found that when the proportion of bottom ash in the recycled ceramic tile specimen increased, the flexural strength of the specimen decreased. However, the majority of them meet the bending strength specifications required for both interior and exterior ceramic tiles. Húlan and Almeida conducted studies on the impact of fly ash on the flexural strength of fired ceramics, including kaolinite, illite, and fly ash (Almeida et al., 2015; Húlan et al., 2020). Fly ash causes shrinkage after firing, a linear decrease in flexural strength with the amount used, and an increase in water absorption. It can be said that the addition of fly ash makes some parameters of ceramics worse. Nonetheless, most studies (Pontikes et al., 2009; Souza et al., 2015; Souza et al., 2016; Yuan et al., 2023) have concluded that fly ash is a suitable admixture for the production of building ceramics.

Fig. 13 shows the correlation between bending strength and water absorption for fly ash or bottom ash tiles. There is a poor linear correlation between bending strength and water absorption, $R^2 = 0.2622$. The correlation between bending strength and water absorption was not obvious with the addition of fly ash or bottom ash.

Table 5. Bending failure and bending strength of coal ash recycled ceramic tile

Test code	Bending failure load (N)	Bending strength (kgf/cm^2)
Control	1944	274.2
10FA	1450	189.2
20FA	1275	157.0
30FA	1018	123.7
40FA	2014	246.7
50FA	1709	209.8
60FA	1617	198.2
10BA	1566	210.6
20BA	1650	213.6
30BA	1398	168.3
40BA	1533	186.0
50BA	1395	158.1
60BA	1148	122.4

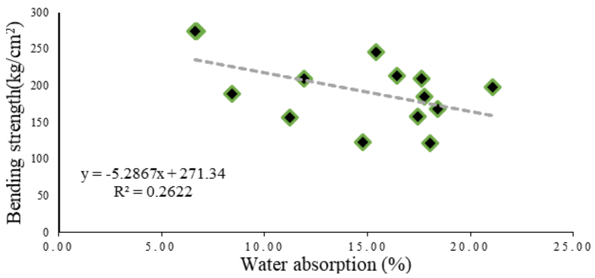

Fig. 13. Correlations between bending strength and water absorption of fly ash or bottom ash ceramic tile

3.6. Results of Thermal Shock Resistance Test

The purpose of the test is to understand the thermal shock resistance of the sintered ceramic tile specimen, and to evaluate the adaptability and durability of the specimen under extreme temperature changes. The test is based on the thermal shock resistance test method of CNS 3299-7 ceramic tile. After experiencing a temperature difference of 110°C in a very short period of time, it is confirmed whether there are any defects on the surface of the ceramic tile specimen. The purpose of dyeing is to make the cracks more visible. The results of the thermal shock resistance test for coal-ash recycled ceramic tile are shown in Table 6.

From Table 6, it can be seen that the fly ash ceramic tile specimens were sintered, dyed, and subjected to thermal shock resistance test, and the state of the specimens was visually observed. From the control group to all fly ash ceramics groups, no cracks were found in the specimens. The sintered fly ash substituted specimens in this study all met the benchmarks of the thermal shock resistance test for ceramic tiles. In addition, the samples replaced by bottom ash did not have any cracks, and the dyeing gradually changed from blue to dark brown as the amount of coal ash increased. The thermal shock test experiences a temperature difference of 110°C in a very short period of time. When the temperature is high, there is no stress on the surface. After rapid cooling, the surface cools first, and the inside becomes a compressed state. The surface is stretched to maintain the balance of forces. Tensile stress can cause cracking (Almeida et al., 2016; Mangi et al., 2022; Yuan et al., 2023). Whether ceramic materials can crack after thermal shock resistance depends on the material's thermal expansion coefficient, thermal conductivity, geometric shape, sintering temperature, etc., which is quite complicated. (Almeida et al., 2016; Faria et al., 2019).

Table 6. Thermal shock resistance of coal ash recycled ceramic tile

Test code	Before dyeing	After dyeing	After test
control			
10FA			
20FA			
30FA			
40FA			
50FA			
60FA			
10BA			
20BA			
30BA			
40BA			
50BA			
60BA			

4. CONCLUSION

This study explores the viability of using coal ash as a partial substitute for specific ceramic raw materials, indicating a sustainable recycling approach. Our key findings are summarized as follows:

(1) As the proportion of coal ash substitution increases, water absorption rates increase, while shrinkage decreases.
(2) Ceramic tile samples with fly ash substitutions ranging from 10% to 60% meet Type III tile standards at 1100°C sintering temperature. Warpage and bending strength tests show promising results, suggesting economic feasibility.
(3) Tiles with 10% bottom ash substitution exhibit optimal water absorption, warpage, and flexural strength, meeting Class II facing brick standards.
(4) Both high-volume fly ash and bottom ash ceramic groups show no cracks post thermal shock resistance testing, confirming their suitability for use.
(5) Warpage values remain below 0.6 mm at 1100°C sintering temperature. However, increased sintering temperature results in warpage values exceeding 1 mm, rendering them unsuitable for wall tiles due to visible irregularities.
(6) Color shifts from blue to dark brown as fly ash or bottom ash proportion increases. Despite this, both groups maintain color integrity post thermal shock resistance testing, indicating potential for blending and coloring purposes.

ACKNOWLEDGMENT

The authors gratefully acknowledge the financial support provided by the Ministry of Science and Technology of Taiwan, grant number [107-2221-E-324-010-MY2].

REFERENCES

Almeida, M.I., Dias, A.C., Demertzi, M., Arroja, L. 2015. Contribution to the development of product category rules for ceramic bricks. Journal of Cleaner Production, 92(1), 206–215.
Almeida, M.I., Dias, A.C., Demertzi, M., Arroja, L. 2016. Environmental profile of ceramic tiles and their potential for improvement. Journal of Cleaner Production, 131(10), 583–593.
Asensio, E., Medina, C., Fras, M., Rojas M. 2020. Fired clay-based construction and demolition waste as pozzolanic addition in cements. Journal of Cleaner Production, 265, 121610.
Babisk, M.P., Amaral, L.F., Ribeiro, L., Vieira, C., Prado, U., Gadioli, M., Oliveira, M., Luz, F., Monteiro, S., Filho, F. 2020. Evaluation and application of sintered red mud and its incorporated clay ceramics as materials for building construction. Journal of Materials Research and Technology, 9(2), 2186–2195.
Bovea, M.D., Saura, Ú., Ferrero, J.L., Giner, J. 2007. Cradle-to-gate study of red clay for use in the ceramic industry. The International Journal of Life Cycle Assessment, 12, 439–447.
Caglayan, H., Caliskan, H. 2018. Energy, exergy and sustainability assessments of a cogeneration system for ceramic industry. Applied Thermal Engineering, 136, 504–515.
Dagnew, E., Hunachew, D. 2022. Alternative resource of incineration bottom ash for ceramic tile production. International Journal of Ceramic Engineering & Science, 4(4), 281–285.
Eduardo, B., Pérez, V.L., Eliche, Q.D., Castro, E. 2018. Manufacture of sustainable clay bricks using waste from secondary aluminum recycling as raw material. Materials, 11, 2439.
Faria, J.S., Manhães, R., Luz, F.S., Monteiro, S.N., Vieira, C.M. 2019. Incorporation of unserviceable tire waste in red ceramic. Journal of Materials Research and Technology, 8(6), 6041–6050.
Gabaldón, E.D., Criado, E., Monfort, E. 2014. The green factor in European manufacturing: A case study of the Spanish ceramic tile industry, Journal of Cleaner Production, 70(1), 242–250.
Glymond, D., Roberts, A., Russell, M., Cheeseman, C. 2018. Production of ceramics from coal furnace bottom ash. Ceramics International, 44, 3009–3014.
Húlan, T., Štubna, I., Ondruška, J. and Trní, A. 2020. The influence of fly ash on mechanical properties of clay-based ceramics. Minerals, 10, 930.
Kummoonin, N., Jaimasith, M., Thiemsorn, W. 2014. Fabrication of ceramic floor tiles from industrial wastes. Warasan Technol Suranaree, 21(2), 65–77.
Mangi, S.A., Raza, M.S., Khahro, S.H. 2022. Recycling of ceramic tiles waste and marble waste in sustainable production of concrete: A review. Environmental Science and Pollution Research, 29, 18311–18332.
Menezes, R., Ferreira, H., Neves, G., Lira, H., Ferreira, H. 2005. Use of granite sawing wastes in the production of ceramic bricks and tiles. Journal of the European Ceramic Society, 25(7), 1149–1158.
Namkane, K., Naksata, W., Thiansem, S., Sooksamiti, P., Arqueropanyo, O. 2017. Utilization of leonardite and coal bottom ash for production of ceramic floor tiles. Environmental Earth Sciences, 76(17), 628.
Ngayakamo, B., Bello, A., Onwualu, A. 2020. Development of eco-friendly fired clay bricks incorporated with granite and eggshell wastes. Environmental Challenges, 1, 100006.
Nicoletti, G.M., Notarnicola, B., Tassielli, G. 2002. Comparative life cycle assessment of flooring materials: Ceramic versus marble tiles. Journal of Cleaner Production, 10, 283–296.
Pontikes, Y., Rathossi, C., Nikoloulos, P., Angelopoulos, G., Jayaseelan, D., Lee, W. 2009. Effect of firing temperature

and atmosphere on sintering of ceramics made from Bayer process bauxite residue. Ceramic International, 35, 401–407.

Schabbach, L., Bolelli, G., Andreola, F., Lancellotti, I., Barbieri, L. 2012. Valorization of MSWI bottom ash through ceramic glazing process: A new technology. Journal of Cleaner Production, 23(1), 147–157.

Sokolar, R.; Smetanova, L. 2010. Dry pressed ceramic tiles based on fly ash-clay body: Influence of fly ash granulometry and pentasodium triphosphate addition. Ceramic International, 36, 215–221.

Souza, A.J., Pinheiro, B., Holanda, J. 2010. Recycling of gneiss rock waste in the manufacture of vitrified floor tiles. Journal of Environmental Management. 91(3), 685–689.

Souza, D., Lafontaine, M., Charron, D.F., Bengoa, X., Chappert, B., Duarte, F. 2015. Comparative life cycle assessment of ceramic versus concrete roof tiles in the Brazilian context. Journal of Cleaner Production, 89, 165–173.

Souza, D., Lafontaine, M., Charron, D.F., Bengoa, X., Chappert, B., Duarte, F. 2016. Comparative life cycle assessment of ceramic brick, concrete brick and cast-in-place reinforced concrete exterior walls, Journal of Cleaner Production, 137, 70–82.

Taurino, R., Karamanov, A., Rosa, R., Karamanova, E., Barbieri, L, Atanasova, V.S. 2017. New ceramic materials from MSWI bottom ash obtained by an innovative microwave-assisted sintering process. Journal of the European Ceramic Society, 37(1), 323–331.

Türkmen, B.A., Özbilen, Ş., Budak, T.D. 2021. Improving the sustainability of ceramic tile production in Turkey. Sustainable Production and Consumption, 27, 2193–2207.

Vieira, A.W., Rosso, L.S., Demarch, A., Pasini, D., Ruzza, S., Arcaro, S., Ribeiro, M., Angioletto, E. 2023. Life cycle assessment in the ceramic tile industry: A review. Journal of Materials Research and Technology, 23, 3904–3915.

Vilarinho, I.S., Filippi, E., Seabra, M.P. 2022. Development of eco-ceramic wall tiles with bio-$CaCO_3$ from eggshells waste. Open Ceramics, 9, 1–9.

Ye, L., Hong, J., Ma, X., Qi, C., Yang, D. 2018. Life cycle environmental and economic assessment of ceramic tile production: a case study in China. Journal of Cleaner Production, 189, 432–441.

Yuan, Q., Robert, D., Mohajerani, A., Tran, P., Pramanik, B. 2023. Sustainable ceramic tiles incorporated with waste fly ash from recycled paper production, Journal of Cleaner Production, 425, 138814.

Zhang, X., Biswas, W.K. 2021. Development of eco-efficient bricks – a life cycle assessment approach. Journal of Building Engineering, 42, 102429.

Zimmer, A., Bergmann, C.P. 2007. Fly ash of mineral coal as ceramic tiles raw material. Journal of Waste Management, 27(1), 59–68.